4. D. R. Klopfenstein, M. Tomishige, N. Stuurman, R. D. Vale, *Cell* **109**, 347 (2002).
5. C. Kural *et al.*, *Science* **308**, 1469 (2005).
6. S. Leibler, D. A. Huse, *J. Cell Biol.* **121**, 1357 (1993).
7. S. A. Endow, H. Higuchi, *Nature* **406**, 913 (2000).
8. M. Badoual, F. Julicher, J. Prost, *Proc. Natl. Acad. Sci. U.S.A.* **99**, 6696 (2002).
9. F. Jülicher, J. Prost, *Phys. Rev. Lett.* **78**, 4510 (1997).
10. S. Camalet, F. Julicher, J. Prost, *J. Phys. Rev. Lett.* **82**, 1590 (1999).
11. S. Camalet, T. Duke, F. Julicher, J. Prost, *Proc. Natl. Acad. Sci. U.S.A.* **97**, 3183 (2000).
12. S. A. Burgess, *J. Mol. Biol.* **250**, 52 (1995).
13. S. P. Gross, Y. Guo, J. E. Martinez, M. A. Welte, *Curr. Biol.* **13**, 1660 (2003).
14. T. Duke, *Philos. Trans. R. Soc. Lond. B Biol. Sci.* **355**, 529 (2000).
15. A. Vilfan, E. Frey, F. Schwabl, *Eur. Phys. J. B* **3**, 535 (1998).
16. Materials and methods are available as supporting material on *Science* Online.
17. J. R. Moll, S. B. Ruvinov, I. Pastan, C. Vinson, *Protein Sci.* **10**, 649 (2001).
18. D. W. Urry, *J. Phys. Chem. B* **101**, 11007 (1997).
19. D. W. Urry *et al.*, *Philos. Trans. R. Soc. Lond. B Biol. Sci.* **357**, 169 (2002).
20. Polymer flexibility can be estimated by calculating the elastic spring constant (κ) of a single ELF_5 linker using data from single molecule force-extension measurements. These experiments yield persistence lengths (L_p) for elastins of $\sim$ 0.4 nm in the low force regime. Assuming a wormlike chain model for the polymer at low extension, κ can be estimated from $\kappa = 3k_bT/2L_pL_c$, where L_c is the contour length of the polymer, k_b is the Boltzman constant, and T is temperature. A single ELF_5 linker contains $\sim$125 amino acids, yielding L_c = 36.35 nm, assuming 0.29 nm per residue, and κ = 0.4 pN/nm.
21. R. B. Case, D. W. Pierce, N. Hom-Booher, C. L. Hart, R. D. Vale, *Cell* **90**, 959 (1997).
22. Y. Inoue, A. H. Iwane, T. Miyai, E. Muto, T. Yanagida, *Biophys. J.* **81**, 2838 (2001).
23. Y. Okada, N. Hirokawa, *Science* **283**, 1152 (1999).
24. Polymer-motor assemblies were formed by making a master mix of K350-Z_E and $(Z_R\text{-}ELF_5)_n$ polymers and incubating for at least 20 min at 4°C before addition to the reaction. Concentrations of polymer solutions were determined from their A_{280} values, using an extinction coefficient of 1480 cm^{-1} mol^{-1} for each Z_R-ELF_5 repeat in the polymers. The fidelity of the assembly process was examined for the trimeric $[K350\text{-}Z_E]_3/(Z_R\text{-}ELF_5)_n$ complex using selectively radiolabeled proteins and multichannel scintillation counting. In these experiments, a K350-Z_E motor was radiolabeled with ^{35}S (77,104 cpm/nmol) by expressing the motor in 1 liter of LB medium supplemented with L-[^{35}S]cysteine (5 mCi). Similarly, a ^3H labeled $(Z_R\text{-}ELF_5)_3$ polymer (33,046 cpm/nmol) was prepared by expression in 0.1 L of LB medium supplemented with L-[3,4(n)-^{3}H]valine (2.5 mCi). After purification, the polymer was functionalized with a PEO-biotinmaleimide (Pierce) using standard maleimide labeling protocols. Then, radiolabeled polymers and motors were mixed in a 1:1.5 ratio with respect to the Z_R sites of the polymer and the motor. After incubation, the [motor]/(polymer) complex was selectively bound to a neutravidin resin. Excess motor was washed from the resin, and the sample, including the resin, was transferred to a scintillation vial. Comparison of the signals from ^{35}S and ^3H channels yielded a motor/polymer ratio of 2.9 $\pm$ 0.4. Control experiments were performed with the polymers omitted from solution; results indicated nonspecific binding of the K350-Z_E motors to the resin did not influence our measurements.
25. D. D. Hackney, *Biophys. J.* **68**, 267s (1995).
26. D. D. Hackney, *Nature* **377**, 448 (1995).
27. W. O. Hancock, J. Howard, *J. Cell Biol.* **140**, 1395 (1998).
28. J. Hyun, W.-K. Lee, N. Nath, A. Chilkoti, S. Zauscher, *J. Am. Chem. Soc.* **126**, 7330 (2004).
29. D. E. Meyer, A. Chilkoti, *Biomacromolecules* **5**, 846 (2004).
30. N. J. Carter, R. A. Cross, *Nature* **435**, 308 (2005).
31. F. H. C. Crick, *Acta Crystallogr.* **6**, 689 (1953).

32. We thank A. J. Link and I. Fushman their help during the early stages of this project; L. Wade and D. Pearson for use of the temperature controller; and P. Wiggins, R. Bao, T. Squires, and S. Quake for valuable discussions. This work was supported by the Beckman Foundation through a Beckman Senior Research Fellowship (to M.R.D.) and by a grant from the National Science Foundation.

Supporting Online Material

www.sciencemag.org/cgi/content/full/311/5766/1468/DC1
Materials and Methods
Table S1
References

2 November 2005; accepted 6 February 2006
10.1126/science.1122125

Progressive Disruption of Cellular Protein Folding in Models of Polyglutamine Diseases

Tali Gidalevitz,* Anat Ben-Zvi,* Kim H. Ho, Heather R. Brignull, Richard I. Morimoto†

Numerous human diseases are associated with the chronic expression of misfolded and aggregation-prone proteins. The expansion of polyglutamine residues in unrelated proteins is associated with the early onset of neurodegenerative disease. To understand how the presence of misfolded proteins leads to cellular dysfunction, we employed *Caenorhabditis elegans* polyglutamine aggregation models. Here, we find that polyglutamine expansions disrupted the global balance of protein folding quality control, resulting in the loss of function of diverse metastable proteins with destabilizing temperature-sensitive mutations. In turn, these proteins, although innocuous under normal physiological conditions, enhanced the aggregation of polyglutamine proteins. Thus, weak folding mutations throughout the genome can function as modifiers of polyglutamine phenotypes and toxicity.

Although many results from in vitro and in vivo models that express mutant Huntingtin, α-synuclein, tau, superoxide dismutase-1, amyloid-β peptide, or prion proteins are consistent with the proposal that non-native species can form toxic folding intermediates, oligomers, and aggregates (*1*–*5*), distinct mechanisms for toxicity have been proposed for each. These mechanisms range from specific protein-protein interactions to disruption of various cellular processes, including transcription (*6*, *7*), protein folding (*8*, *9*), protein clearance (*10*–*13*), energy metabolism (*14*), activation of apoptotic pathways (*15*), and others. This has led us to consider how the expression of a single aggregation-prone protein could have such pleiotropic effects and whether a more general mechanism could explain the many common features of protein conformation diseases. Moreover, because each cell and tissue contains various metastable polymorphic proteins (*16*), could the chronic expression of an aggregation-prone protein have global consequences on homeostasis and thus affect folding or stability of proteins that harbor folding defects?

To test this hypothesis, we took a genetic approach using diverse *Caenorhabditis elegans* temperature-sensitive (ts) mutations to examine whether the functionality of the respective protein at the permissive condition was affected by expression of aggregation-prone polyglutamine (polyQ) expansions. Because many ts mutant proteins are highly dependent on the cellular folding environment (*17*–*19*), they represent highly sensitive indicators of a disruption in protein homeostasis. We employed transgenic *C. elegans* lines expressing different-length polyQ-YFP (yellow fluorescent protein) or CFP (cyan fluorescent protein) from integrated arrays in muscle (polyQm) (*20*, *21*) or neuronal (polyQn) (*22*) cells. Both models show polyQ-length–dependent aggregation and toxicity.

Animals expressing ts mutant UNC-15 (*C. elegans* homolog of a muscle paramyosin) were crossed to *C. elegans* polyQm strains, and phenotypes at permissive and restrictive conditions were examined in double homozygotes. At the restrictive temperature, this ts mutation disrupts thick filament formation and leads to embryonic and early larval lethality and slow movement in adults (*23*). Expression of polyQ proteins alone in a wild-type background did not result in these embryonic and larval phenotypes. In contrast, more than 40% of embryos coexpressing mutant paramyosin and Q40m [paramyosin(ts)+Q40m] failed to hatch or

Department of Biochemistry, Molecular Biology, and Cell Biology, Rice Institute for Biomedical Research, Northwestern University, Evanston, IL 60208, USA.

*These authors contributed equally to this work.
†To whom correspondence should be addressed. E-mail: r-morimoto@northwestern.edu

move at the permissive temperature (Fig. 1, A and C). This effect was polyQ-length–dependent, because coexpression of Q35m or Q24m with paramyosin(ts) resulted in 27% or 5% unhatched embryos, respectively (Fig. 1C). The morphology of affected paramyosin(ts)+Q40m and paramyosin(ts)+Q35m embryos at 15°C (Fig. 1A) was similar to paramyosin(ts) at 25°C (Fig. 1B). Examination of muscle structure in paramyosin(ts)+Q40m embryos at 15°C revealed a disrupted pattern of actin staining, similar to the pattern in paramyosin(ts) embryos at 25°C but not at 15°C (fig. S1) or in wild-type animals (*24*). Thus, expression of an aggregation-prone polyQ protein is sufficient to cause a paramyosin ts mutation to exhibit its mutant phenotype at the permissive condition.

We next addressed whether this effect of polyQ expansions extended to neuronal cells, which are often affected in conformational diseases. Animals expressing a ts mutation in the neuronal protein dynamin-1 [dynamin(ts) animals] become paralyzed at the restrictive temperature (28°C) but have normal motility at the permissive temperature (20°C) (*25*). Pan-neuronal expression of Q40 in dynamin(ts) animals resulted in severe impairment of mobility (Fig. 1D) at the permissive temperature. No phenotypes were observed in animals coexpressing the nonaggregating Q19n. Thus, expression of polyglutamine expansions phenocopies temperature-sensitive mutations in muscle and neuronal cells at permissive conditions, and this genetic interaction reflects the aggregation propensity of polyQ expansions.

To ask whether these observations were applicable to other ts mutations, we tested the genetic interaction of Q40m and Q24m proteins with a wide range of characterized ts mutations (Table 1). Strains expressing ts mutant proteins UNC-54, UNC-52, LET-60 (*C. elegans* homologs of myosin, perlecan, and ras-1, respectively), or UNC-45 together with Q24m or Q40m were scored for specific ts phenotypes (*26*) at the permissive temperature. For all lines generated, the ts mutant phenotype was exposed at permissive conditions in the presence of the aggregation-prone Q40m but not by nonaggregating Q24m (Table 1). Thus, the chronic expression of an aggregation-prone polyQ protein interferes with the function of multiple structurally and functionally unrelated proteins.

To test whether interaction between polyQ expansions and ts mutant proteins was cell autonomous, we took advantage of tissue-specific phenotypes caused by expression of ras(ts) protein at the restrictive temperature: an embryonic lethality/larval development phenotype (Let/Lva), a defect in osmoregulation (Osm) likely reflecting neuronal dysfunction, and a multivulva phenotype (Muv) resulting from dysfunction in the hypodermis (*27*). We scored these phenotypes upon expression of polyQ in neuronal or muscle cells. PolyQ expansions in neurons led to exposure of the Osm phenotype in ras(ts) animals at the permissive temperature but had no effect on the Let/Lva phenotype (Fig. 1E). Conversely, heterozygous expression of Q40m in muscle cells of ras(ts) animals caused 48% penetrance of Let/Lva phenotype but did not expose the neuronal Osm phenotype (Fig. 1E). Double homozygous ras(ts)+Q40m animals could not be scored, as they did not reach mature adulthood (Table 1) (*26*). Neither neuronal nor muscle cell expression of polyQ expansions caused the hypodermal Muv phenotype (*24*). A similar control was performed with paramyosin(ts), which was not affected by polyQ expansions in neurons (Q67n) (*24*). Likewise, polyQ expansions did not affect Unc phenotypes that did not involve ts proteins (caused either by RNAi or gene deletion) (*24*).

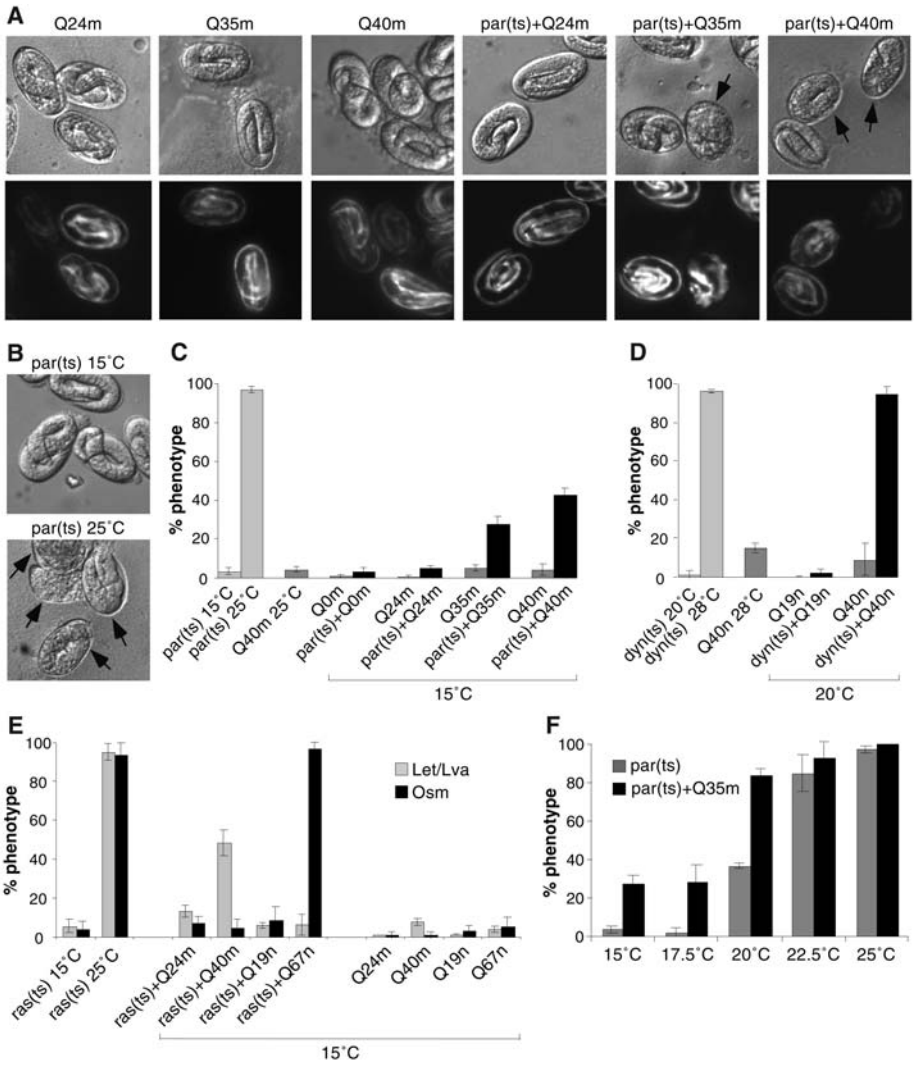

Fig. 1. Aggregation-prone proteins expose temperature-sensitive phenotypes of paramyosin(ts) (A to C, and F), dynamin(ts) (D), and ras(ts) (E) mutants at permissive temperatures. (**A**) Differential interference contrast (DIC) and fluorescent images of age-synchronized 3-fold embryos at 15°C. Fluorescence shows expression of polyQm (muscle)-YFP proteins (Q0m, Q24m, Q35m, and Q40m) from the unc-54 promoter. Arrows indicate embryos with abnormal body shape. (**B**) DIC images of age-synchronized 3-fold paramyosin(ts) embryos at indicated temperatures. Arrows as in (A). (**C**) Percentage of unhatched embryos and paralyzed L1 larvae. Data are the mean ± SD, ≥380 embryos per data point. (**D**) Percentage of uncoordinated age-synchronized young adult animals. Expression of polyQn (neuronal)-YFP proteins (Q19n, Q40n) is from the F25B3.3 promoter. Data are the mean ± SD, ≥80 animals per data point. (**E**) Percentage of animals exhibiting either Osm (black) or the combined Let/Lva (gray) phenotypes. Expression of Q67n is from the F25B3.3 promoter. Data are the mean ± SD, ≥70 synchronized adults for Osm and ≥270 embryos for Let/Lva. ras(ts)+Q40m denotes ras(ts) animals heterozygous for Q40m. (**F**) Synergistic effect of elevated temperature and polyQ expansions on paramyosin(ts). Percentage of unhatched embryos and paralyzed L1 larvae for paramyosin(ts) (gray) and paramyosin(ts)+Q35m (black) at indicated temperatures. Data are the mean ± SD, ≥300 embryos for each data point.

Table 1. PolyQ expansions affect the functionality of unrelated ts mutant proteins. Specific phenotype of each ts mutation alone or in polyQm background was scored at indicated temperatures (*26*). Data are the mean ± SD for at least the indicated number (*n*) of animals for each phenotype scored. *See (*26*).

Proteins expressed	TS allele	Phenotype scored (*n* value)	Animals displaying phenotype (%)			
			15°C	25°C	15°C	
					Q24	Q40
PolyQm	–	Slow movement ($n > 300$)			6.0 ± 5.3	4.6 ± 4.2
myosin(ts)	e1301		5.6 ± 2.6	84.7 ± 13.5		
myosin(ts)+Qm	e1301				11.2 ± 6.7	51.9 ± 19.3
myosin(ts)	e1157		5 ± 4	98.7 ± 1.4		
myosin(ts)+Qm	e1157				5.9 ± 1.5	55 ± 6
PolyQm	–	Abnormal body shape			0	0
perlecan(ts)	su250	(stiff paralysis) ($n > 100$)	1 ± 1.2	97.6 ± 2.2		
perlecan(ts)+Qm	su250				0.8 ± 1.1	48.4 ± 6.5
PolyQm	–	Egg-laying defect ($n > 85$)			0	0
UNC-45(ts)	e286		8.4 ± 2.1	93.8 ± 4.9		
UNC-45(ts)+Qm	e286				5.1 ± 7.3	87.7 ± 8.1
PolyQm	–	Embryonic lethality + larval			1 ± 0.15	7.9 ± 1.8
ras(ts)	ga89	development arrest ($n > 270$)	5.6 ± 3.4	95.2 ± 4.3		
ras(ts)+Qm	ga89				13.3 ± 3	100*

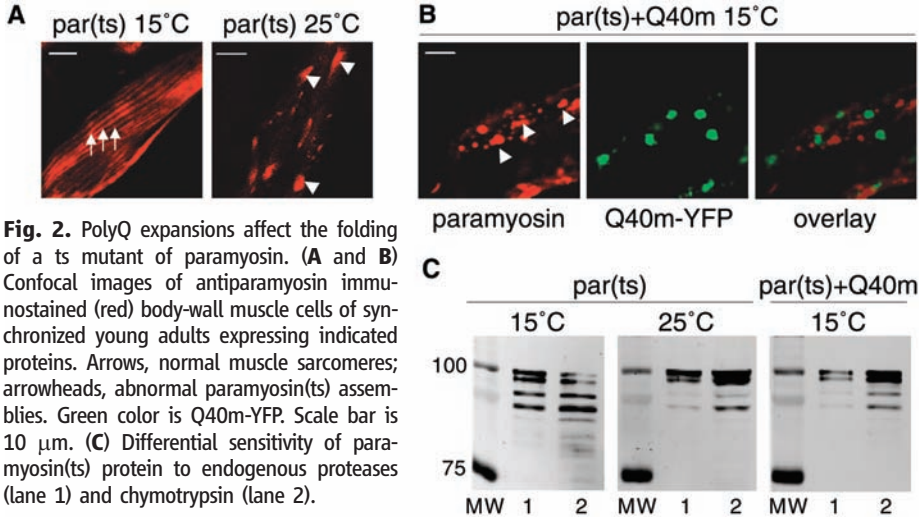

Fig. 2. PolyQ expansions affect the folding of a ts mutant of paramyosin. (**A** and **B**) Confocal images of antiparamyosin immunostained (red) body-wall muscle cells of synchronized young adults expressing indicated proteins. Arrows, normal muscle sarcomeres; arrowheads, abnormal paramyosin(ts) assemblies. Green color is Q40m-YFP. Scale bar is 10 μm. (**C**) Differential sensitivity of paramyosin(ts) protein to endogenous proteases (lane 1) and chymotrypsin (lane 2).

Thus, the effect of polyQ expansions on mutant ts proteins reflects specific genetic interactions within the same cell type and does not result from decreased fitness of the organism.

To understand the nature of this interaction, we examined the localization of paramyosin(ts) protein coexpressed with Q40m. The L799F mutation affects coiled-coil interactions in paramyosin and at restrictive temperature results in mislocalization to paracrystalline assemblies instead of muscle sarcomeres (Fig. 2A) (*23*). Paramyosin(ts) protein coexpressed with Q40m at permissive conditions assembled into abnormal paracrystalline structures, distinct from the Q40m aggregates (Fig. 2B), and exhibited altered protease sensitivity (Fig. 2C). Thus, expression of Q40m uncovers the protein folding defect in paramyosin(ts) mutant. In view of this, the differential penetrance of ts phenotypes (Table 1) may reflect the sensitivity of each ts mutation to disruption of the folding environment.

Aggregation-prone proteins may thus exert their destabilizing effects by placing a stress on the folding capacity of the cell. If so, the elevated temperature and the presence of aggregation-prone protein may synergize in their destabilizing effects on ts mutants. Expression of an intermediate length (Q35m) expansion shifted the temperature at which paramyosin(ts) was fully inactivated (Fig. 1F). Next, we asked whether the difference in penetrance from 48% to 100% Let/Lva phenotype of ras(ts) animals in the heterozygous and homozygous Q40m backgrounds (Table 1 and Fig. 1E) could be explained by differences in aggregation of Q40m. Heterozygous Q40m animals consistently showed later onset of aggregation and lower numbers of aggregates than homozygous animals (Fig. 3, A, B, and E). If the levels of polyQ affect the folding of the ts protein, does the misfolding of the ts protein, in turn, intensify misfolding of polyQ? Q40m aggregation in paramyosin(ts) and ras(ts) backgrounds was enhanced dramatically (Fig. 3, C to E). In contrast, loss of function mutations not associated with expression of ts proteins (for example in paramyosin or perlecan) did not enhance aggregation (*24*). From a genetic perspective, temperature-sensitive mutations in proteins unrelated to cellular folding or clearance pathways behaved as modifiers of polyQ aggregation. Thus, a positive feedback mechanism exists to enhance the disruption of cellular folding homeostasis.

The appearance of misfolded protein in the cell normally activates a stress response that increases protein refolding and turnover and thus rebalances the folding environment (*28*, *29*). In contrast, our results point to the unexpected sensitivity of cellular folding homeostasis to the chronic expression of misfolded proteins under physiological conditions. It is possible that the low flux of misfolded protein in conformational diseases may alone lack the capacity to activate the homeostatic stress response. This suggests that the stress response fails to compensate for the chronic expression of misfolded proteins in human disease.

One potential interpretation of our results is that the protein folding capacity of the cell, integrated at a systems level, is a reflection of expressed protein polymorphisms and random mutations (*16*), which in themselves do not lead to disease because of the balance achieved by folding and clearance mechanisms. However, these proteins may misfold and in turn contribute to the progressive disruption of the folding environment when this balance becomes overwhelmed, e.g., by the expression of an aggregation-prone protein in conformational diseases. Our data identify the presence of mar-

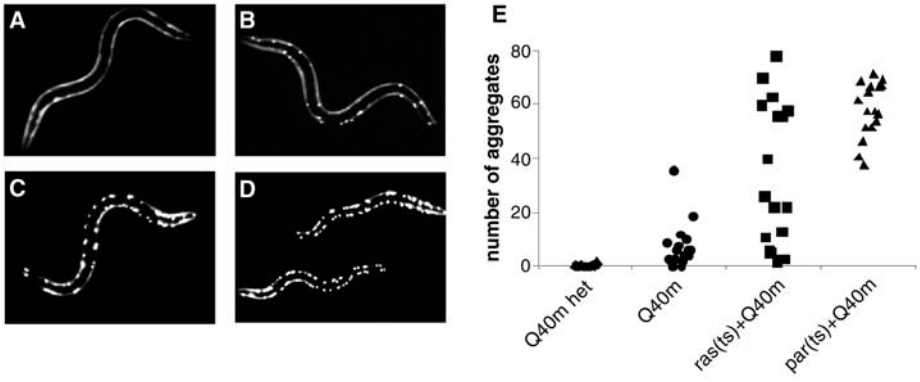

Fig. 3. Progressive disruption of cellular folding capacity by misfolded proteins. (**A** to **D**) Fluorescent images of representative L2 larvae at the permissive temperature of heterozygous (A) or homozygous (B) Q40m, ras(ts)+Q40m (C), and paramyosin(ts)+Q40m (D) strains. (**E**) Number of visible aggregates in L2 larvae expressing indicated proteins. ras(ts)+Q40m in (C) and (E) denotes the fluorescent progeny of an F2 ras(ts) animal expressing Q40m; these progeny could be either homozygous or heterozygous for Q40m.

ginally stable or folding-defective proteins in the genetic background of conformational diseases as potent extrinsic factors that modify aggregation and toxicity. Given the prevalence of polymorphisms in the human genome (*30*), they could contribute to variability of disease onset and progression (*31*). This interpretation also provides a mechanistic basis to the notion that the late onset of protein misfolding diseases may be due to gradual accumulation of damaged proteins (*32*), resulting in a compromise in folding capacity. Indeed, in a screen for regulators of polyQ aggregation in *C. elegans*, we identified nearly 200 genes whose diverse functions have the potential to affect protein homeostasis (*21*). Cellular degeneration in diseases of protein conformation is unlikely to be due to a single defect. Thus, the many toxic effects on various cellular processes attributed to misfolded proteins (*6*–*15*) could in fact be an integral part of the global disruption of protein homeostasis identified in this work.

References and Notes

1. S. W. Davies *et al.*, *Cell* **90**, 537 (1997).
2. M. DiFiglia *et al.*, *Science* **277**, 1990 (1997).
3. R. Kayed *et al.*, *Science* **300**, 486 (2003).
4. M. Tanaka, P. Chien, N. Naber, R. Cooke, J. S. Weissman, *Nature* **428**, 323 (2004).
5. J. F. Gusella, M. E. MacDonald, *Nat. Rev. Neurosci.* **1**, 109 (2000).
6. M. K. Perez *et al.*, *J. Cell Biol.* **143**, 1457 (1998).
7. A. McCampbell *et al.*, *Hum. Mol. Genet.* **9**, 2197 (2000).
8. P. J. Muchowski *et al.*, *Proc. Natl. Acad. Sci. U.S.A.* **97**, 7841 (2000).
9. S. Kim, E. A. A. Nollen, K. Kitagawa, V. P. Bindokas, R. I. Morimoto, *Nat. Cell Biol.* **4**, 826 (2002).
10. K. Ii, H. Ito, K. Tanaka, A. Hirano, *J. Neuropathol. Exp. Neurol.* **56**, 125 (1997).
11. C. J. Cummings *et al.*, *Nat. Genet.* **19**, 148 (1998).
12. N. F. Bence, R. M. Sampat, R. R. Kopito, *Science* **292**, 1552 (2001).
13. C. I. Holmberg, K. E. Staniszewski, K. N. Mensah, A. Matouschek, R. I. Morimoto, *EMBO J.* **23**, 4307 (2004).
14. M. Gu *et al.*, *Ann. Neurol.* **39**, 385 (1996).
15. V. L. Gabai, A. B. Meriin, J. A. Yaglom, V. Z. Volloch, M. Y. Sherman, *FEBS Lett.* **438**, 1 (1998).
16. S. L. Rutherford, S. Lindquist, *Nature* **396**, 336 (1998).
17. T. K. Van Dyk, A. A. Gatenby, R. A. LaRossa, *Nature* **342**, 451 (1989).
18. C. R. Brown, L. Q. Hong-Brown, W. J. Welch, *J. Clin. Invest.* **99**, 1432 (1997).
19. C. B. Pedersen *et al.*, *J. Biol. Chem.* **278**, 47449 (2003).
20. J. F. Morley, H. R. Brignull, J. J. Weyers, R. I. Morimoto, *Proc. Natl. Acad. Sci. U.S.A.* **99**, 10417 (2002).
21. E. A. Nollen *et al.*, *Proc. Natl. Acad. Sci. U.S.A.* **101**, 6403 (2004).
22. H. R. Brignull, S. Tang, R. I. Morimoto, in preparation.
23. K. Gengyo-Ando, H. Kagawa, *J. Mol. Biol.* **219**, 429 (1991).
24. Gidalevitz *et al.*, unpublished data.
25. S. G. Clark, D. L. Shurland, E. M. Meyerowitz, C. I. Bargmann, A. M. van der Bliek, *Proc. Natl. Acad. Sci. U.S.A.* **94**, 10438 (1997).
26. Materials and methods are available as supporting material on *Science* Online.
27. D. M. Eisenmann, S. K. Kim, *Genetics* **146**, 553 (1997).
28. S. A. Goff, A. L. Goldberg, *Cell* **41**, 587 (1985).
29. R. I. Morimoto, *Genes Dev.* **12**, 3788 (1998).
30. International SNP Map Working Group, *Nature* **409**, 928 (2001).
31. U.S.-Venezuela Collaborative Research Project, N. S. Wexler, *Proc. Natl. Acad. Sci. U.S.A.* **101**, 3498 (2004).
32. C. N. Oliver, B. W. Ahn, E. J. Moerman, S. Goldstein, E. R. Stadtman, *J. Biol. Chem.* **262**, 5488 (1987).

33. T.G. was supported by NIH Training Grant T32 HL076139 and by an Individual NRSA F32 GM075583-01; A.B.-Z. was supported by an EMBO Long-Term Fellowship, the Parkinson Foundation, and the Hereditary Disease Foundation; and H.R.B. was supported by National Institute of General Medical Sciences (NIGMS) Molecular Biology of Disease Training Grant T32 GM08061. R.I.M. was supported by grants from the NIH (NIGMS, National Institute of Neurological Disorders and Stroke, and National Institute on Aging), the Huntington Disease Society of America Coalition for the Cure, the ALS Association, and the Daniel F. and Ada L. Rice Foundation. Some nematode strains used in this work were provided by the Caenorhabditis Genetics Center, which is funded by the NIH National Center for Research Resources (NCRR). We thank J. West and members of the Morimoto laboratory for their discussion and comments on the manuscript and F. Moore for reagents.

Supporting Online Material

www.sciencemag.org/cgi/content/full/1124514/DC1
Materials and Methods
Fig. S1
References

3 January 2006; accepted 16 January 2006
Published online 9 February 2006;
10.1126/science.1124514
Include this information when citing this paper.

The Global Impact of Scaling Up HIV/AIDS Prevention Programs in Low- and Middle-Income Countries

John Stover,[1] Stefano Bertozzi,[2] Juan-Pablo Gutierrez,[2] Neff Walker,[3] Karen A. Stanecki,[4] Robert Greener,[4] Eleanor Gouws,[4] Catherine Hankins,[4] Geoff P. Garnett,[5] Joshua A. Salomon,[6] J. Ties Boerma,[7] Paul De Lay,[4] Peter D. Ghys[4]*

A strong, global commitment to expanded prevention programs targeted at sexual transmission and transmission among injecting drug users, started now, could avert 28 million new HIV infections between 2005 and 2015. This figure is more than half of the new infections that might otherwise occur during that period in 125 low- and middle-income countries. Although preventing these new infections would require investing about U.S.$122 billion over this period, it would reduce future needs for treatment and care. Our analysis suggests that it will cost about U.S.$3900 to prevent each new infection, but that this will produce a savings of U.S.$4700 in forgone treatment and care costs. Thus, greater spending on prevention now would not only prevent more than half the new infections that would occur from 2005 to 2015 but would actually produce a net financial saving as future costs for treatment and care are averted.

Much has changed in the global response to the AIDS epidemic since the late 1990s. Access to treatment and care in the developing world was limited by costs, by the complexity of early treatment regimens, and by a perceived lack of capacity to implement treatment programs even if drug costs were greatly reduced. The pioneering work of Brazil in providing broad access to antiretroviral therapy proved that, with political